

# A description of the finite differencing used by the B-grid dynamical core

Bruce Wyman

NOAA/GFDL

— August 21, 2003 —

## 1 Introduction

This paper describes the dynamical part of a global, hydrostatic grid point model developed from models described in Mesinger et al. (1988) and Wyman (1996). The model described here solves the same set of dynamical equations but has a modified vertical and horizontal grid. The vertical grid is a hybrid sigma-pressure coordinate system, sigma coordinate surfaces in the lower model levels may gradually transform to pressure coordinate surfaces in the upper model levels. The horizontal grid has been switched to the Arakawa B-grid (Arakawa and Lamb 1977). This has several advantages over the previously used E-grid configuration, especially in the global domain, where the convergence of diagonal fluxes near the pole of the E-grid has been eliminated in the B-grid. An additional benefit is the simplification of model output, a single field on the B-grid is essentially on its own rectangular A-grid. The basic time differencing schemes used has not changed from either of the preceding models. The step-mountain (eta) coordinate is no longer a supported option, although much of the code remains in place, very little effort has been made to ensure that it works correctly.

This paper will describe the finite difference schemes used to solve the dynamical equations on the global B-grid. This will include descriptions of the time differencing, horizontal mixing, lateral boundary conditions, and polar filtering.

## 2 The horizontal grid

The prognostic variables on the semi-staggered Arakawa B-grid lie on two overlapping grids. The momentum components ( $u$  and  $v$ ) are located together on what will be called the *momentum* or *velocity grid*. Surface pressure ( $p_s$ ), temperature ( $T$ ), and an arbitrary number of tracers ( $R$ ) are located together on what will be called the *mass* or *temperature grid*. The momentum and mass grids are rectangular in shape, with equal spacing in longitude ( $\lambda$ )

along the x-axis and latitude ( $\varphi$ ) along the y-axis. The grids are diagonally shifted from each other, such that, the center of a momentum grid box is located at the corner where four mass grid boxes intersect.

Auxiliary grids can be defined for computing additional quantities. The zonal mass flux grid (or **U** grid) has grid boxes centered on the east and west faces of a mass grid box. The meridional mass flux grid (or **V** grid) has grid boxes centered on the north and south faces of a mass grid box.

Horizontal indexing increases from west to east, and from south to north. Figure 1 shows the indexing scheme used by the various grids. Indexing is set up so that a velocity grid box with the same  $i,j$  is centered at the northeast corner of a mass (temperature) grid box, while the grid box  $\mathbf{U}_{i,j}$  is centered on the east face, and the grid box  $\mathbf{V}_{i,j}$  is centered on the north face.

If the grid spacing along the x- and y-axis is given as  $\Delta\lambda$  and  $\Delta\varphi$ , respectively, then using spherical geometry the grid distance in meters can be defined as

$$\Delta x = a \Delta\lambda \frac{\delta_\varphi \sin \varphi}{\Delta\varphi} \quad (2.1a)$$

$$\Delta y = a \Delta\varphi \quad (2.1b)$$

where  $a$  is the radius of the earth. Then the area of temperature and velocity grid boxes is computed as

$$A_t = \Delta x_t \Delta y \quad (2.2a)$$

$$A_v = \Delta x_v \Delta y \quad (2.2b)$$

The global grid is aligned so that velocity grid boxes are centered on the equator and at the poles. The temperature grid will have grid box edges line up with the equator and poles, therefore the global temperature grid must have an even number of latitude grid boxes.

### 3 The vertical coordinate

The model uses a sigma/pressure hybrid vertical coordinate. Near the Earth's surface model levels are defined only by the terrain-following sigma coordinate. In upper model layers, well above the topography, the coordinate surfaces may coincide with constant pressure surfaces. In between there is a slow transition from sigma to pressure.

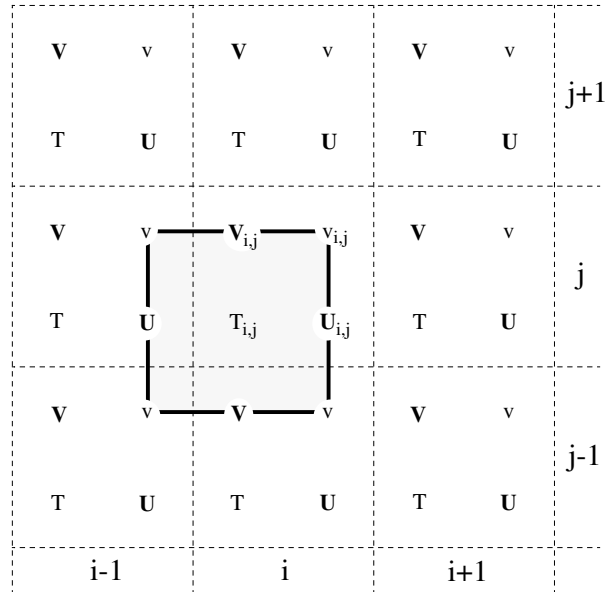


Figure 1: The indexing and relative locations of the four sub-grids. The surface pressure, temperature, and tracers are located on the temperature grid (T points), momentum is located on the velocity grid (v points), and the zonal and meridional mass fluxes are located at U and V points. The heavy line denotes the boundaries of a temperature grid box.

The model variables  $u$ ,  $v$ ,  $T$ , and  $R$  are grid box averages, essentially located at full model levels. Vertical velocity is diagnosed at the interface between model layers. Vertical indexing increases from the top of the atmosphere towards the surface.

### 3.1 Pressure at half levels

The B-grid model uses a vertical differencing scheme similar to that described by Simmons and Burridge (1981). The vertical coordinate is defined by a reference profile of pressure  $P$  and sigma/eta values  $\eta$  at the half-model levels. The pressure at half levels can be computed from the surface pressure  $p_s$  as

$$p_{k+\frac{1}{2}} = P_{k+\frac{1}{2}} + \eta_{k+\frac{1}{2}} p_{sl} \quad (3.1)$$

For the sigma coordinate case,  $p_{sl} = p_s$ , and for the eta coordinate case,  $p_{sl} = p_s/\eta_s$ . Here  $\eta_s$  is the sigma/eta value at the Earth's surface. For the special case of a pure sigma coordinate,  $P = 0$  (at all levels). When defining the vertical profile of  $P$  and  $\eta$ , the following conditions must be met

$$\eta_{\frac{1}{2}} = 0 \quad (3.2a)$$

$$\eta_{N+\frac{1}{2}} = 1 \quad (3.2b)$$

$$P_{surface} = 0 \quad (3.2c)$$

If there are  $N$  model levels, then pressure is computed at half levels from  $p_{\frac{1}{2}}$  to  $p_{N+\frac{1}{2}}$ . Again, for the sigma coordinate case,  $p_{N+\frac{1}{2}} = p_s$ .

The sigma coordinate with a non-zero pressure at the top of the model is a special case of the hybrid coordinate. The reference profile of pressures can be computed from  $\eta$ -values and  $p_{top} \neq 0$ .

$$P_{k+\frac{1}{2}} = p_{top} (1 - \eta_{k+\frac{1}{2}}) \quad (3.3)$$

### 3.2 Pressure thickness

The mass weight for individual model layers is computed from the pressure at half model levels as

$$\Delta p_k = \delta_\eta p = p_{k+\frac{1}{2}} - p_{k-\frac{1}{2}} \quad (3.4)$$

### 3.3 Pressure at full levels

The pressure at full model levels is computed as in Simmons and Burridge (Equation 3.18) in a manner that is consistent with the pressure gradient term (5.11).

$$\ln p_k = \frac{p_{k+\frac{1}{2}} \ln p_{k+\frac{1}{2}} - p_{k-\frac{1}{2}} \ln p_{k-\frac{1}{2}}}{\Delta p_k} - 1 \quad (3.5)$$

## 4 The equations

The fundamental quantities predicted by the model are the momentum components, surface pressure, temperature, and tracers. The prognostic equations written for the vertical coordinate eta ( $\eta$ ) follow that of Wyman (1996), Mesinger et al. (1988), and Mesinger (1984). The equations for momentum, temperature, and tracers can be written respectively as

$$\frac{d\vec{v}}{dt} + f\vec{k} \times \vec{v} + \nabla\Phi + \frac{R_d T^*}{p} \nabla p + \vec{F} = 0 \quad (4.1a)$$

$$\frac{dT}{dt} + \frac{1}{c_p} \frac{R_d T^*}{p} \left[ \int_0^\eta (\nabla \cdot \frac{\partial p}{\partial \eta} \vec{v}) d\eta - (\vec{v} \cdot \nabla p) \right] + F_T = 0 \quad (4.1b)$$

$$\frac{dr}{dt} + F_r = 0 \quad (4.1c)$$

The continuity equation is given as

$$\frac{\partial}{\partial \eta} \left( \frac{\partial p}{\partial t} \right) + \nabla \cdot \vec{v} \frac{\partial p}{\partial \eta} + \frac{\partial}{\partial \eta} \left( \dot{\eta} \frac{\partial p}{\partial \eta} \right) = 0. \quad (4.2)$$

The velocity of the vertical coordinate surface  $\dot{\eta} \equiv \frac{d\eta}{dt}$ , is computed by integrating (4.2)

$$\dot{\eta} \frac{\partial p}{\partial \eta} = -\frac{\partial p}{\partial t} - \int_0^\eta (\nabla \cdot \frac{\partial p}{\partial \eta} \vec{v}) d\eta \quad (4.3)$$

where the surface pressure tendency is

$$\frac{\partial p_s}{\partial t} = - \int_0^{\eta_s} (\nabla \cdot \frac{\partial p}{\partial \eta} \vec{v}) d\eta. \quad (4.4)$$

Geopotential height  $\Phi$  in (4.1a), is determined by integrating the hydrostatic equation

$$\frac{\partial \Phi}{\partial \eta} = -\frac{R_d T^*}{p} \frac{\partial p}{\partial \eta} \quad (4.5)$$

where  $R_d$  is the gas constant for dry air,  $T^*$  is the virtual temperature (defined later) and  $p$  is the pressure.

The Coriolis and curvature terms in (4.1a) are defined as  $f = 2\Omega \sin \phi + (u/a) \tan \phi$ , where  $a$  and  $\Omega$  are the radius and angular speed of rotation of the earth, respectively.  $\vec{F}$ ,  $F_T$ ,

and  $F_r$  represent the mixing terms for momentum, temperature and tracers, respectively. This paper will only discuss the lateral mixing terms, the vertical terms are considered part of the physical parameterizations.

## 5 Finite differencing

### 5.1 The adjustment terms

#### 5.1.1 Mass divergence

The mass divergence is computed at model levels and on the temperature grid as

$$D_k = \frac{1}{A_t} (\delta_\lambda \mathbf{U} + \delta_\varphi \mathbf{V})_k \quad (5.1)$$

The horizontal mass fluxes in (5.1) are computed at the east and north faces of a temperature grid box as

$$\mathbf{U}_k = \overline{u_k \Delta y \Delta p_k^v}^\varphi \quad (5.2a)$$

$$\mathbf{V}_k = \overline{v_k \Delta x_v \Delta p_k^v}^\lambda \quad (5.2b)$$

The pressure thickness at velocity points  $\Delta p_k^v$  is computed by taking an area weighted average of pressure thickness from the four surrounding overlapping mass grid boxes.

$$\Delta p_k^v = \frac{\sum_1^4 a_v \Delta p_k}{A_v} \quad (5.3)$$

Here  $a_v$  is the area of overlap of a mass grid box with a velocity grid box, where  $\sum_1^4 a_v = A_v$ .

#### 5.1.2 Surface pressure tendency

The surface pressure tendency (4.4) is computed by integrating the mass divergence (5.1) from the top of the atmosphere to the surface.

$$\frac{\partial p_s}{\partial t} = - \sum_{k=1}^N D_k \quad (5.4)$$

### 5.1.3 Vertical velocity

The vertical mass flux is computed at half levels on the mass grid as

$$\mathbf{W}_{k+\frac{1}{2}} = (\dot{\eta}p_s)_{k+\frac{1}{2}} = - \left( \eta_{k+\frac{1}{2}} \frac{\partial p_s}{\partial t} + \eta_s \sum_{n=1}^N D_n \right). \quad (5.5)$$

where the vertical velocity,  $\dot{\eta} = \frac{d\eta}{dt}$ .

### 5.1.4 Hydrostatic equation

Geopotential height at half and full levels is computed by integrating the hydrostatic equation (4.5) up from the surface.

$$\Phi_{k-\frac{1}{2}} = \Phi_{k+\frac{1}{2}} + R_d T_k^* (w_k^b + w_k^a) \quad (5.6a)$$

$$\Phi_k = \Phi_{k+\frac{1}{2}} + R_d T_k^* w_k^b \quad (5.6b)$$

The lower boundary condition is the surface height  $\Phi_s$ .

$$\Phi_{N+\frac{1}{2}} = \Phi_s \quad (5.7)$$

If the model has moisture, the virtual temperature is computed as

$$T_k^* = T_k \left( 1 + \frac{R_v - R_d}{R_d} Q_k \right) \quad (5.8)$$

where  $R_d$  is the gas constant for dry air,  $R_v$  is the gas constant for water vapor, and  $Q_k$  is specific humidity (a tracer field). For a dry model,  $T_k^* = T_k$ .

The weights in (5.6) are computed from the pressure at half and full model levels.

$$w_k^a = \ln p_k - \ln p_{k-\frac{1}{2}} \quad (5.9a)$$

$$w_k^b = \ln p_{k+\frac{1}{2}} - \ln p_k \quad (5.9b)$$

Here,  $w_k^b$  is equivalent to  $\alpha_k$  in Simmons and Burridge (1981). Using these weights, the finite difference form of the hydrostatic equation (5.6) reduces to the usual form  $\delta\Phi = R_d T^* \delta \ln p$ .

### 5.1.5 Pressure gradient term

The term  $\nabla p/p$  in (4.1a) and (4.1b) is computed in a manner consistent with Simmons and Burridge (1981). The zonal and meridional components are computed on model levels and

at mass flux points ( $\mathbf{U}$ ,  $\mathbf{V}$  points) as

$$(C_\lambda)_k = \frac{1}{\overline{\Delta p_k}^\lambda} (\overline{w_k^a}^\lambda \delta_\lambda p_{k-\frac{1}{2}} + \overline{w_k^b}^\lambda \delta_\lambda p_{k+\frac{1}{2}}) \quad (5.10a)$$

$$(C_\varphi)_k = \frac{1}{\overline{\Delta p_k}^\varphi} (\overline{w_k^a}^\varphi \delta_\varphi p_{k-\frac{1}{2}} + \overline{w_k^b}^\varphi \delta_\varphi p_{k+\frac{1}{2}}) \quad (5.10b)$$

The average meridional pressure thickness is computed using an area-weighted average similar to (5.3).

$$\overline{\Delta p_k}^\varphi = \frac{(2a_v \Delta p_k)_{north} + (2a_v \Delta p_k)_{south}}{A_v}$$

### 5.1.6 Pressure gradient force

The pressure gradient force, the third and fourth term on the LHS of Equation (4.1a), can be computed in one of two ways: using the Simmons and Burridge (1981) scheme or the Lin (1997) finite-volume integration method. With both schemes the implementation for the B-grid is similar. First, pressure gradient components are computed on the east/west and north/south faces of the velocity grid boxes. (This is essentially computing the pressure gradient on the C-grid.) Then, these components are averaged to the middle of a B-grid velocity grid box.

#### Simmons and Burridge scheme

For the Simmons and Burridge scheme the geopotential height evaluated at full model levels (5.6b) and the pressure gradient terms (5.10) are used. The pressure gradient components at the faces of a velocity grid box are computed as

$$(P_\lambda)_k = (\delta_\lambda \Phi)_k + \overline{R_d T_k^*}^\lambda (C_\lambda)_k \quad (5.11a)$$

$$(P_\varphi)_k = (\delta_\varphi \Phi)_k + \overline{R_d T_k^*}^\varphi (C_\varphi)_k \quad (5.11b)$$

These components are then averaged to momentum grid boxes to get the pressure gradient force components on the B-grid.

$$(G_\lambda)_k = -\frac{1}{\Delta x_v} (\overline{P_\lambda}^\varphi)_k \quad (5.12a)$$

$$(G_\varphi)_k = -\frac{1}{\Delta y} (\overline{P_\varphi}^\lambda)_k \quad (5.12b)$$

## Finite volume scheme

The scheme computes a contour integral of the pressure forces acting on the finite volume. The pressure gradient force for the x-z plane as given by Lin (Equation 10) is

$$\frac{du}{dt} = \frac{\int_c \bar{\Phi} d \ln p}{\int_c \overline{\ln p} dx} \quad (5.13)$$

The B-grid implementation evaluates the numerator and denominator at **U** and **V** points and then separately averages the integrals to the middle of a velocity grid box. Only the pressure and geopotential height at half model levels (5.6a) are needed. The contour integrals in the numerator and denominator of (5.13) can be computed as

$$(Num_\lambda)_k = \delta_\lambda(\bar{\Phi}^\eta \delta_\eta \ln p) - \delta_\eta(\bar{\Phi}^\lambda \delta_\lambda \ln p) \quad (5.14a)$$

$$(Denom_\lambda)_k = -\delta_\eta \overline{\ln p}^\lambda \Delta x \quad (5.14b)$$

and for the meridional component as

$$(Num_\varphi)_k = \delta_\varphi(\bar{\Phi}^\eta \delta_\eta \ln p) - \delta_\eta(\bar{\Phi}^\varphi \delta_\varphi \ln p) \quad (5.15a)$$

$$(Denom_\varphi)_k = -\delta_\eta \overline{\ln p}^\varphi \Delta y \quad (5.15b)$$

The numerator and denominator are then separately averaged to momentum grid boxes to get the pressure gradient force components for the B-grid.

$$(G_\lambda)_k = \frac{(\overline{Num_\lambda}^\varphi)_k}{(\overline{Denom_\lambda}^\varphi)_k} \quad (5.16a)$$

$$(G_\varphi)_k = \frac{(\overline{Num_\varphi}^\lambda)_k}{(\overline{Denom_\varphi}^\lambda)_k} \quad (5.16b)$$

It should be noted that the Lin scheme does not use the pressure gradient terms (5.10), which are used for cancellation with the horizontal omega-alpha term (5.17). Therefore, conservation of energy between the pressure gradient and omega-alpha term is not guaranteed with the Lin finite volume pressure gradient.

### 5.1.7 Omega-alpha term

The omega-alpha term is represented by the second term on the LHS of Equation (4.1b). There are two parts to this term (in the square brackets), the horizontal gradient of pressure and vertical integral of divergence. The horizontal part of the omega-alpha term averages the horizontal mass fluxes (5.2) and  $\nabla p/p$  term (5.10) to temperature points. The vertical

part evaluates the integral of divergence at model levels using the pressure weights (5.9). This may be expressed in finite difference form as

$$\left(\frac{\omega}{p}\right)_k = \frac{1}{\Delta p_k} \left[ \frac{1}{A_t} (\overline{UC}_\lambda^\lambda + \overline{VC}_\varphi^\varphi)_k + (w_k^a \sum_{n=1}^{k-1} D_n + w_k^b \sum_{n=1}^k D_n) \right] \quad (5.17)$$

The temperature tendency is then computed as

$$\left(\frac{\partial T_k}{\partial t}\right)_{\omega\alpha} = \frac{R_d T_k^*}{c_p} \left(\frac{\omega}{p}\right)_k \quad (5.18)$$

### 5.1.8 Divergence damping

When taking long atmospheric time steps, the physics tendencies may produce high amplitude, small scale noise, or so called grid point storms. Divergence damping (Sadourney 1975) may be used to reduce or eliminate these small scale disturbances. The damping is applied to the momentum components by taking the gradient of the divergence. This type of scheme provides only second order damping and is quite dissipative. The model described here has extended the scheme to a fourth-order scheme that more selectively damps smaller scales. The scheme as applied to the momentum tendencies can be expressed as

$$\left(\frac{\partial u}{\partial t}\right)_{ddamp} = K^* \frac{1}{\Delta t} \frac{\Delta x}{\Delta p} \overline{\delta_\lambda D^*}^\varphi \quad (5.19a)$$

$$\left(\frac{\partial v}{\partial t}\right)_{ddamp} = K^* \frac{1}{\Delta t} \frac{\Delta y}{\Delta p} \overline{\delta_\varphi D^*}^\lambda \quad (5.19b)$$

When the scheme is second order,  $D^*$  is the divergence and  $K^* = \frac{K_{ddamp}}{8}$ , where  $K_{ddamp}$  is a user specified coefficient. For the fourth order scheme,

$$D^* = \delta_\lambda \delta_\lambda D + \delta_\varphi \delta_\varphi D \quad (5.20)$$

where  $D$  is the divergence and  $K^* = -\frac{K_{ddamp}}{64}$ .

The user specified coefficient has been normalized by the maximum allowable value and should be in the range,  $0 \leq K_{ddamp} \leq 1$ . In the current implementation,  $K_{ddamp}$  is set to 1 at one latitude row adjacent to the pole when the divergence damping term is non-zero. This helps dissipate numerical noise related to the polar boundary.

## 5.2 The advection terms

### 5.2.1 Advection

The advective tendencies are computed separately for the horizontal plane and the vertical axis. The default spatial differencing is centered (either second or fourth-order), and there is an option for vertical tendencies to be computed by a finite volume scheme using either a piecewise linear scheme (Lin et al. 1994) or piecewise parabolic method (PPM) (Colella and Woodward 1984). The finite volume advection schemes are described in another report.

The advective tendencies are computed in flux form then adjusted using the pressure tendency. Using temperature as an example, this may be represented as

$$\left(\frac{\partial T_k}{\partial t}\right)_{adv} = \frac{1}{\Delta p_k} \left[ \frac{\partial \Delta p_k T_k}{\partial t} - T_k \frac{\partial \Delta p_k}{\partial t} \right] \quad (5.21)$$

The first term in brackets on the RHS represents the advective tendency in flux form. If the second term contains the pressure tendency over the advective time step, then the global average mass-weighted temperature will be conserved. The same procedure is used for prognostic tracers and momentum. For non-prognostic tracers, those that are not advected, the tendency in flux form is zero but the pressure adjustment term must still be computed to account for changes in surface pressure. The details of the time differencing will be explained later.

The horizontal and vertical tendencies for temperature (shown) or tracers in flux form is computed as

$$\left(\frac{\partial \Delta p_k T_k}{\partial t}\right)_{horiz} = -\frac{1}{A_t} \left[ \delta_\lambda (\mathbf{U} \hat{T}^\lambda) + \delta_\varphi (\mathbf{V} \hat{T}^\varphi) \right]_k \quad (5.22)$$

$$\left(\frac{\partial \Delta p_k T_k}{\partial t}\right)_{vert} = - \left[ (\mathbf{W} \hat{T}^\eta)_{k+\frac{1}{2}} - (\mathbf{W} \hat{T}^\eta)_{k-\frac{1}{2}} \right] \quad (5.23)$$

where

$$\hat{T}^\lambda = \alpha_2 \bar{T}^\lambda + \alpha_4 \bar{T}^{3\lambda} \quad (5.24a)$$

$$\hat{T}^\varphi = \alpha_2 \bar{T}^\varphi + \alpha_4 \bar{T}^{3\varphi} \quad (5.24b)$$

$$\hat{T}^\eta = \alpha_2 \bar{T}^\eta + \alpha_4 \bar{T}^{3\eta} \quad (5.24c)$$

The operators  $\bar{T}^\lambda$ ,  $\bar{T}^\varphi$ , and  $\bar{T}^\eta$  are simple averages of temperatures at adjacent grid point. The operators  $\bar{T}^{3\lambda}$ ,  $\bar{T}^{3\varphi}$ , and  $\bar{T}^{3\eta}$  are averages of temperature over three grid intervals. The coefficients  $\alpha_2$  and  $\alpha_4$  control the second-order and fourth-order schemes. For the second-order scheme,  $\alpha_2 = 1$  and  $\alpha_4 = 0$ . For the fourth-order scheme,  $\alpha_2 = 7/6$  and  $\alpha_4 = -1/6$ .

It should be noted that a more accurate vertical average value for  $\widehat{T}^\eta$  can be determined using the thickness of the model layers, however, this type of weighted-average will not conserve energy.

The advective tendencies for momentum in flux form are computed in a manner identical to temperature (except the mass fluxes are averaged to the appropriate grid points).

$$\left(\frac{\partial \Delta p_k^v v_k}{\partial t}\right)_{horiz} = -\frac{1}{A_t} \left[ \delta_\lambda (\overline{\mathbf{U}}^{\lambda\varphi} \widehat{v}^\lambda) + \delta_\varphi (\overline{\mathbf{V}}^{\lambda\varphi} \widehat{v}^\varphi) \right]_k \quad (5.25)$$

$$\left(\frac{\partial \Delta p_k^v v_k}{\partial t}\right)_{vert} = - \left[ (\overline{\mathbf{W}}^{\lambda\varphi} \widehat{v}^\eta)_{k+\frac{1}{2}} - (\overline{\mathbf{W}}^{\lambda\varphi} \widehat{v}^\eta)_{k-\frac{1}{2}} \right] \quad (5.26)$$

Here,  $\overline{\mathbf{U}}^{\lambda\varphi}$  and  $\overline{\mathbf{V}}^{\lambda\varphi}$  are simple four-point averages of the horizontal mass fluxes (5.2) and  $\overline{\mathbf{W}}^{\lambda\varphi}$  is a four-point area-weighted average of the vertical mass flux (5.5).

### 5.2.2 Horizontal mixing

Horizontal mixing is computed using a second-order smoothing operator applied along coordinate surfaces. The result from the second-order operator may be reapplied to achieve higher order mixing. The second-order operator for temperature (or prognostic tracers) is computed as

$$M^2(T) = \frac{1}{A_t \Delta p_k} [\delta_\lambda (K_\lambda \delta_\lambda T) + \delta_\varphi (K_\varphi \delta_\varphi T)] \quad (5.27)$$

The zonal and meridional coefficients are

$$K_\lambda = K_T \Delta_\lambda \overline{A_t}^\lambda \overline{\Delta p_k}^\lambda \quad (5.28a)$$

$$K_\varphi = K_T \Delta_\varphi \overline{A_t}^\varphi \overline{\Delta p_k}^\varphi \quad (5.28b)$$

where  $\overline{A_t}^\lambda$ ,  $\overline{A_t}^\varphi$ ,  $\overline{\Delta p_k}^\lambda$ , and  $\overline{\Delta p_k}^\varphi$  are simple two-point averages along the appropriate axis.  $K_T$  is a user specified non-dimensional mixing coefficient for temperature,  $0 \leq K_T \leq 1$ , and  $\Delta_\lambda$  and  $\Delta_\varphi$  are constants that describe the strength of the mixing with latitude. For the mixing to remain stable the condition,  $K_T \Delta_\lambda \leq 1/8$  and  $K_T \Delta_\varphi \leq 1/8$ , must be met. A unique  $K_T$  may be specified for all variables.

Fourth-order mixing is computed by reapplying the the result from the second-order operator (for sixth-order mixing the fourth-order operator is reapplied). The fourth-order mixing for temperature can be expressed as

$$\left(\frac{\partial T}{\partial t}\right)_{hdiff} = \frac{1}{\Delta t} M^4(T) \approx -\frac{1}{\Delta t} [M^2(M^2(T))] \quad (5.29)$$

The mixing of momentum is handled analogous to temperature.

The second-order operator for momentum is computed as

$$M^2(v) = \frac{1}{A_v \Delta p_k^v} [\delta_\lambda (K_\lambda \delta_\lambda v) + \delta_\varphi (K_\varphi \delta_\varphi v)] \quad (5.30)$$

with zonal and meridional coefficients of

$$K_\lambda = K_v \Delta_\lambda^v \overline{A_v^\lambda} \overline{\Delta p_k^{v\lambda}} \quad (5.31a)$$

$$K_\varphi = K_v \Delta_\varphi^v \overline{A_v^\varphi} \overline{\Delta p_k^{v\varphi}} \quad (5.31b)$$

where  $\overline{A_v^\lambda}$ ,  $\overline{A_v^\varphi}$ ,  $\overline{\Delta p_k^{v\lambda}}$ , and  $\overline{\Delta p_k^{v\varphi}}$  are defined the same as the similar terms in (5.28).  $K_v$  is a user specified non-dimensional mixing coefficient for momentum and the condition:  $K_v \Delta_\lambda^v \leq 1/8$  and  $K_v \Delta_\varphi^v \leq 1/8$ , must be met.

The schemes that specify  $\Delta_\lambda$ ,  $\Delta_\varphi$ ,  $\Delta_\lambda^v$ , and  $\Delta_\varphi^v$  as functions of latitude are defined in the Appendix.

### 5.2.3 Horizontal mixing slope correction

Horizontal mixing along terrain following coordinate surfaces may introduce large errors in regions with steep topographic slopes. These errors may be especially noticeable for temperature and some tracers fields (such as moisture) where the spurious mixing up sloping model surfaces may lead to large maxima (in quantities such as precipitation) in high mountainous regions.

To adjust for this effect a correction may be added to the zonal and meridional fluxes of horizontal mixing.

For temperature this correction is computed as

$$s_\lambda = -\frac{\overline{\gamma_k^T}^\lambda}{\gamma_k^T} \delta_\lambda p_k \quad (5.32a)$$

$$s_\varphi = -\frac{\overline{\gamma_k^T}^\varphi}{\gamma_k^T} \delta_\varphi p_k \quad (5.32b)$$

where

$$\gamma_k^T = \frac{T_{k+1} - T_{k-1}}{p_{k+1} - p_{k-1}} \quad (5.33)$$

At the top and bottom levels one-sided differences are used.

The slope corrections  $s_\lambda$  and  $s_\varphi$  are added into the zonal and meridional fluxes in the temperature/tracer mixing equation (5.27).

$$M^2(T) = \frac{1}{A_t \Delta p_k} [\delta_\lambda (K_\lambda (\delta_\lambda T + K_s s_\lambda)) + \delta_\varphi (K_\varphi (\delta_\varphi T + K_s s_\varphi))] \quad (5.34)$$

where  $0 \leq K_s \leq 1$ , is a user specified coefficient for the slope correction.  $K_s$  may be set as a global background value and as separate values for each of the three lowest model levels. It is recommended that  $K_s \ll 1$  at the lowest model level due to the one-side estimate of  $\gamma_k^T$  in a typically thin sigma layer near the surface. If fourth-order (or higher) mixing is used the slope correction is only applied to the first pass of the second-order operator.

#### 5.2.4 Filling negative tracer values

Negative tracer values can be generated by several different terms. The advection of tracers using centered differencing schemes may be the largest contributor to negative tracer. Also the use of polar filtering with the centered difference advection scheme is a very large contributor in high latitudes. Another less obvious source of negative tracer is higher-order horizontal mixing. The second-order smoothing operator does not create negative tracer, but the fourth-order or higher schemes can create negative tracer when there are very sharp gradients.

With semi-Lagrangian finite-volume advection schemes the source of negative tracer is limited to truncation errors. There is no need for polar filtering and with the implicit diffusion of the schemes, there is typically no need for horizontal mixing.

The negative tracer filling schemes used in this model borrow from the nearest grid points in the vertical and horizontal in a way that conserves the global tracer mass. The schemes are applied to each prognostic tracer separately.

#### Vertical borrowing

Vertical borrowing is performed after advection. Equal parts are borrowed from adjacent grid points below and above.

First, compute the deficit ( $D_k$ ) and surplus ( $S_k$ ) at all levels

$$D_k = \min(\Delta p_k R_k, 0)$$

$$S_k = \max(\Delta p_k R_k, 0)$$

Then, starting at the top of the model and proceeding down through all model levels compute an adjustment where there is a deficit ( $D_k < 0$ ).

The fraction of the available surplus from adjacent levels is

$$F_k = \max\left(\frac{S_{k-1} + S_{k+1}}{-D_k}, 1\right)$$

Compute the contribution from the level above  $R^u$  and the level below  $R^b$

$$R^u = S_{k-1}/F_k$$

$$R^b = S_{k+1}/F_k$$

then compute the adjustment to the tracer at level  $k$  and adjacent levels

$$\begin{aligned}\Delta_t R_k &= \frac{1}{\Delta p_k} (R^u + R^b) \\ \Delta_t R_{k-1} &= -\frac{1}{\Delta p_{k-1}} R^u \\ \Delta_t R_{k+1} &= -\frac{1}{\Delta p_{k+1}} R^b\end{aligned}\tag{5.35}$$

also modifying the surplus at the level below

$$S_{k+1} = S_{k+1} - R^b\tag{5.36}$$

The tracer tendency for vertical borrowing is computed from (5.35) as

$$\left(\frac{\partial R_k}{\partial t}\right)_{vfill} = \frac{1}{\Delta t} \Delta_t R_k\tag{5.37}$$

### Horizontal borrowing

A modified smoothing scheme is used that is similar to horizontal mixing. A second-order operator, essentially a five-point Shapiro filter, is repetitively applied to borrow from neighboring grid points.

The second-order operator at level  $k$  is computed as

$$\delta_t R_k = \frac{1}{A_t \Delta p_k} [\delta_\lambda (K_\lambda \delta_\lambda R_k) + \delta_\varphi (K_\varphi \delta_\varphi R_k)]\tag{5.38}$$

The zonal and meridional coefficients are

$$\begin{aligned}K_\lambda &= \frac{1}{8} \overline{A_t}^\lambda \overline{\Delta p_k}^\lambda \\ K_\varphi &= \frac{1}{8} \overline{A_t}^\varphi \overline{\Delta p_k}^\varphi\end{aligned}$$

where the terms  $\overline{(\ )}^\lambda$  and  $\overline{(\ )}^\varphi$  are simple two-point averages along the appropriate axis. The horizontal borrowing scheme sets coefficients  $K_\lambda$  and  $K_\varphi$  to zero where borrowing should not occur. In other words,  $K_\lambda$  will be non-zero when the adjacent tracers values (in  $\delta_\lambda R$ ) have opposite signs.

If successive second order passes are applied, the non-zero flux coefficients from previous passes are not reset to zero. This allows for better filling of large negative regions. The tracer tendency for horizontal borrowing is computed from (5.38) as

$$\left(\frac{\partial R_k}{\partial t}\right)_{fill} = \frac{1}{\Delta t} \delta_t R_k \quad (5.39)$$

### 5.2.5 Sponge layer

A one-layer sponge may be applied at the top level of the model. The sponge performs strong eddy damping of the prognostic fields. The damping is done using a 5-point Shapiro filter, similar to that used for horizontal mixing and tracer hole filling. For temperature, tracers, and zonal wind the zonal mean is removed before applying the filter. For the meridional wind, the entire field is damped.

The following formula is used

$$\left(\frac{\partial \vartheta}{\partial t}\right)_{sponge} = \frac{K_{sp}}{A_t \Delta p_k \Delta t} [\delta_\lambda (K_\lambda \delta_\lambda \vartheta) + \delta_\varphi (K_\varphi \delta_\varphi \vartheta)] \quad (5.40)$$

where  $\vartheta = T^*$ ,  $R^*$ ,  $u^*$ , or  $v$ ; note that  $(\ )^*$  represents that the zonal mean has been removed.  $K_{sp}$  is a user-specified damping coefficient, where  $0 \leq K_{sp} \leq 1$ . The zonal and meridional coefficients are

$$K_\lambda = \frac{1}{8} \overline{A_t}^\lambda \overline{\Delta p_k}^\lambda$$

$$K_\varphi = \frac{1}{8} \overline{A_t}^\varphi \overline{\Delta p_k}^\varphi$$

where  $\overline{(\ )}^\lambda$  and  $\overline{(\ )}^\varphi$  are again simple two-point averages along the appropriate axis.

*In practice, it is usually sufficient to apply the sponge to only the momentum components.*

## 6 Time differencing

### 6.1 Adjustment terms

The model is integrated using a two time-level scheme. Gravity waves use the forward-backward scheme (Mesinger 1977), in which the surface pressure is integrated with a forward step and the Coriolis and pressure gradient terms with a backward step.

The forward step for surface pressure and temperature can be represented as

$$p_s^{\tau+1} = p_s^\tau + \Delta t \left( \frac{\partial p_s}{\partial t} \right)^\tau \quad (6.1)$$

$$T^{\tau+1} = T^\tau + \Delta t \frac{(R_d T_k^*)^\tau}{c_p} \left( \frac{\omega}{p} \right)^\tau \quad (6.2)$$

where all terms on the RHS are computed using time level  $\tau$ .

The backward step for momentum can be represented as

$$u^{\tau+1} = u^\tau + \Delta t C_\lambda - \Delta t G_\lambda^{\tau+1}$$

$$v^{\tau+1} = v^\tau + \Delta t C_\varphi - \Delta t G_\lambda^{\tau+1}$$

The pressure gradient  $G$  is computed using the mass fields at time level  $\tau + 1$ . The Coriolis terms  $C_\lambda$  and  $C_\varphi$  are solved using a modified trapezoidal implicit scheme.

$$C_\lambda = f^\tau [(1 - \alpha)v^\tau + \alpha v^{\tau+1}]$$

$$C_\varphi = -f^\tau [(1 - \alpha)u^\tau + \alpha u^{\tau+1}]$$

$$f = 2\Omega \sin \varphi + (u^\tau/a) \tan \varphi$$

The scheme is explicit when  $\alpha = 0$ , implicit when  $\alpha = 1$ , and equivalent to the trapezoidal scheme when  $\alpha = \frac{1}{2}$  (currently the default).

## 6.2 Advection terms

Since explicit time differencing for advection is unstable for the two-time level scheme, a modified Euler-backward scheme is used instead (Matsuno 1966). Furthermore, additive split time differencing is used so that a longer advective time step can be taken (Gadd 1978).

The modified Euler-backward scheme is a two-step scheme, using the temperature/tracer advection equation (5.21) this can be represented as:

### Step 1

$$T_k^+ = T_k^\tau + \Delta t \frac{\partial T_k}{\partial t} \quad (6.3)$$

$$\frac{\partial T_k^*}{\partial t}_g = \frac{1}{\Delta p_k^{\tau+1}} \left[ \frac{\partial \Delta p_k T_k^{\tau+}}{\partial t} - T_k^{\tau a} \frac{\Delta p_k^{\tau+1} - \Delta p_k^{\tau a}}{\Delta t} \right] \quad (6.4)$$

### Step 2

$$T_k^* = T_k^\tau + \Delta t \left[ \frac{\partial T_k}{\partial t} + w \frac{\partial T_k^*}{\partial t}_g \right] \quad (6.5)$$

$$\left(\frac{\partial T_k}{\partial t}\right)_{adv} = \frac{1}{\Delta p_k^{\tau+1}} \left[ \frac{\partial \Delta p_k T_k^*}{\partial t} - T_k^{\tau_a} \frac{\Delta p_k^{\tau+1} - \Delta p_k^{\tau_a}}{\Delta t} \right] \quad (6.6)$$

In the first step, an initial temperature  $T_k^+$  is computed from the current temperature tendency and then used to compute a first guess of the advective tendency. In the second step, an estimate of the future temperature  $T_k^*$  is computed using the advective tendency from step 1. The final part of step 2 computes the final advective tendency using the estimate of the future temperature.

In step 2, the weight factor must be,  $0 \leq w \leq 1$ . If  $w = 0$  the scheme reduces to the standard Euler-forward scheme, which is unstable, and if  $w = 1$  the scheme is the full Euler-backward scheme. When  $w < 1$ , the modified scheme has less damping than the full Euler-backward scheme (personal communication, F. Mesinger; also see Kurihara and Tripoli 1976).

The time-splitting of adjustment and advection time step is accomplished by summing the mass fluxes ( $\mathbf{U}, \mathbf{V}, \mathbf{W}$ ) over adjustment time steps and by saving the values for  $\Delta p_k$ ,  $u$ ,  $v$ , and  $T$  from the previous advection time step ( $\tau_a$ ). Because tracers are only updated on the advection time step there is no need to save the previous value. Note that with this scheme the advection time step must be a multiple of the adjustment time step.

The tracer filling, horizontal mixing, and the top level sponge are all computed using values at time level  $\tau + 1$ .

## 7 Lateral Boundaries

The global compute domain is defined as the set of grid points where the model's prognostic variables are computed. Additional rows of grid points called halo rows (or points) extend beyond all four lateral boundaries of the global compute domain to make it easier to calculate the horizontal finite differencing.

Data in halo rows are assigned values based on data in the compute domain. Halo rows that are beyond the east and west boundaries of the global compute domain are assigned values using cyclic continuity. While halo rows to the north and south must be assigned values that allow cross-polar flow and retain the conservation properties of the numerical schemes (i.e., the conservation of mass and total energy).

The row of momentum grid boxes at the pole is considered a halo row. The momentum components at pole row  $p$  are set as

$$u_{i,p} = v_{i,p} = 0 \quad (7.1)$$

Data in halo rows that are beyond the pole row (outside the global compute domain) are assigned values based on data in the compute domain.

$$u_{i,p+n} = u_{i,p-n} \quad (7.2a)$$

$$v_{i,p+n} = -v_{i,p-n} \quad (7.2b)$$

$$T_{i,p+n} = T_{i,p-n} \quad (7.2c)$$

$$R_{i,p+n} = R_{i,p-n} \quad (7.2d)$$

## 8 Polar filtering

A polar filtering scheme is used at high latitudes to damp the shortest resolvable waves so that a longer time step can be taken. Filtering is applied to the mass divergence, horizontal omega-alpha tendency, horizontal advective tendency of temperature and prognostic tracers, and the momentum components. The momentum components are transformed to stereographic coordinates before they are filtered to minimize distortion near the poles. The filtering scheme conserves mass and tracer mass, but does not conserve energy (Takacs and Balgovid 1983).

The fields are filtered by transforming a full latitude circle of data to Fourier components using a fast Fourier transform (FFT). The Fourier components are damped (i.e., multiplied) by a given function of wave number and latitude, and then transformed back to grid point space using the inverse FFT. The polar filter function used for damping the Fourier components is related to wave number  $k$ , and latitude row  $j$ , and is defined as

$$S_{j,k} = \left( \frac{\cos \varphi_j}{\cos \varphi_{ref}} \frac{1}{\sin X} \right)^m \quad (8.1)$$

where  $0 \leq S_{j,k} \leq 1$ ,  $X = k\Delta\lambda/2$ , and  $\cos \varphi_{ref}$  is the reference latitude poleward of which filtering is performed. Typically filtering is done poleward of 60 degrees latitude, but this is an adjustable model parameter. The strength of the filter increases with higher wave numbers and latitude. The factor  $m$  is an optional parameter for increasing the overall strength of the filter when additional stability is needed, the default is  $m = 1$ .

## 9 Energy conservation

The numerical schemes and finite differencing used in this model have been designed to conserve mass, kinetic and potential energy, and total energy. Exceptions to this include the

time differencing and the diffusive terms: polar filtering, horizontal mixing, and the sponge. (The finite volume pressure gradient is also not guaranteed to conserve energy.) For the most part the non-energy conservation is small, and for relatively short model integrations is not important. For longer climate simulations a correction may be computed to account for this lack of exact energy conservation.

The conservation of total energy can be expressed as the summation over all grid points and model levels of the time rate of change of kinetic energy (KE) and potential energy (PE).

$$\sum \frac{\partial KE \Delta p}{\partial t} \Delta x \Delta y + \sum \frac{\partial PE \Delta p}{\partial t} \Delta x \Delta y = 0 \quad (9.1)$$

The residual from (9.1) is used to compute a correction term to the temperature. The correction is uniform at all grid points and model levels.

$$\frac{\partial T}{\partial t} = \frac{- \left[ \frac{1}{c_p} \sum \frac{\partial KE \Delta p}{\partial t} \Delta x \Delta y + \sum \frac{\partial PE \Delta p}{\partial t} \Delta x \Delta y \right]}{\sum \Delta x \Delta y \Delta p} \quad (9.2)$$

The kinetic energy contribution is computed as

$$\frac{\partial KE \Delta p}{\partial t} = \left[ (u^\tau + \frac{1}{2} \Delta t \frac{\partial u}{\partial t}) \frac{\partial u}{\partial t} + (v^\tau + \frac{1}{2} \Delta t \frac{\partial v}{\partial t}) \frac{\partial v}{\partial t} \right] \Delta p^{\tau+1} + \frac{1}{2} (u^2 + v^2)^\tau \frac{\partial \Delta p}{\partial t} \quad (9.3)$$

and the potential energy contribution as

$$\frac{\partial PE \Delta p}{\partial t} = \frac{1}{c_p} \left[ \frac{\partial T}{\partial t} \Delta p^{\tau+1} + T^\tau \frac{\partial \Delta p}{\partial t} \right] \quad (9.4)$$

## A Notation

The operator  $\delta_s A$  represents the simple difference between adjacent grid points along the  $s$ -axis. Similarly, the operator  $\overline{A}^s$  represents the simple average between adjacent grid points along the  $s$ -axis. Using the stencil in Figure 1, the following differencing can be derived.

For  $A$  at  $T$  (or  $\mathbf{V}$ ) points the operators evaluated along the x-axis at  $\mathbf{U}$  (or  $v$ ) points are defined

$$\begin{aligned}(\delta_\lambda A)_{i,j} &= A_{i+1,j} - A_{i,j} \\ (\overline{A}^\lambda)_{i,j} &= A_{i+1,j} + A_{i,j}\end{aligned}$$

and evaluated along the y-axis at  $\mathbf{V}$  (or  $v$ ) points are defined

$$\begin{aligned}(\delta_\varphi A)_{i,j} &= A_{i,j+1} - A_{i,j} \\ (\overline{A}^\varphi)_{i,j} &= A_{i,j+1} + A_{i,j}\end{aligned}$$

For  $A$  at  $v$  (or  $\mathbf{U}$ ) points the operators evaluated along the x-axis at  $\mathbf{V}$  (or  $T$ ) points are defined

$$\begin{aligned}(\delta_\lambda A)_{i,j} &= A_{i,j} - A_{i-1,j} \\ (\overline{A}^\lambda)_{i,j} &= A_{i,j} + A_{i-1,j}\end{aligned}$$

and evaluated along the y-axis at  $\mathbf{U}$  (or  $T$ ) points are defined

$$\begin{aligned}(\delta_\varphi A)_{i,j} &= A_{i,j} - A_{i,j-1} \\ (\overline{A}^\varphi)_{i,j} &= A_{i,j} + A_{i,j-1}\end{aligned}$$

The operators for vertical differencing are defined

$$\begin{aligned}(\delta_\eta A)_{i,j,k} &= A_{i,j,k+1} - A_{i,j,k} \\ (\overline{A}^\eta)_{i,j,k} &= A_{i,j,k+1} + A_{i,j,k}\end{aligned}$$

## B Horizontal mixing coefficients

The latitudinal strength of the horizontal mixing is determined by  $\Delta_\lambda$  and  $\Delta_\varphi$  in (5.28), and by  $\Delta_\lambda^v$  and  $\Delta_\varphi^v$  in (5.31). The variation of mixing with latitude can be controlled by

five possible schemes. Scheme 1 has globally uniform mixing, schemes 2-5 provide increased mixing towards the poles.

**Scheme 1:** Uniform mixing

$$\Delta_\lambda = \Delta_\varphi = \frac{1}{8}$$

**Scheme 2:** Increased mixing poleward of latitude  $\varphi_{ref}$ .

$$\Delta_\lambda = \Delta_\varphi = \frac{1}{8} \text{MAX} \left( 1, \frac{\Delta x_{eq}^2 + \Delta y^2}{\frac{\Delta x^2}{\cos^2 \varphi_{ref}} + \Delta y^2} \right)$$

**Scheme 3:** Larger increase in mixing poleward of latitude  $\varphi_{ref}$ .

$$\Delta_\lambda = \Delta_\varphi = \frac{1}{8} \text{MAX} \left( 1, \frac{\Delta x_{ref}^2}{\Delta x^2} \right)$$

**Scheme 4:** Increased mixing poleward of latitude  $\varphi_{ref}$ , but only along x-axis.

$$\Delta_\lambda = \frac{1}{8} \text{MAX} \left( 1, \frac{\Delta x_{eq}^2 + \Delta y^2}{\frac{\Delta x^2}{\cos^2 \varphi_{ref}} + \Delta y^2} \right)$$

$$\Delta_\varphi = \frac{1}{8}$$

**Scheme 5:** Larger increase in mixing poleward of latitude  $\varphi_{ref}$ , but only along x-axis.

$$\Delta_\lambda = \frac{1}{8} \text{MAX} \left( 1, \frac{\Delta x_{ref}^2}{\Delta x^2} \right)$$

$$\Delta_\varphi = \frac{1}{8}$$

In schemes 2-5,  $\varphi_{ref}$  is the latitude at which the poleward increase in mixing begins, equatorward of this latitude there is uniform mixing (equivalent to scheme 1).  $\Delta x$  and  $\Delta y$  are defined by (2.1a) and (2.1b),  $\Delta x_{eq}$  is defined at the equator, and  $\Delta x_{ref}$  is defined at the reference latitude ( $\varphi_{ref}$ ).

## References

- Arakawa, A. and V. R. Lamb, 1977: Computational design of the basic dynamical processes of the UCLA general circulation model. *Methods in Computational Physics*, Vol. 17. Academic Press, 173–265.
- Colella, P. and P. R. Woodward, 1984: The piecewise parabolic method (PPM) for gas-dynamical simulations. *J. Comput. Phys.*, **54**, 174–201.
- Gadd, A. J., 1978: A split explicit integration scheme for numerical weather prediction. *Quart. J. Roy. Meteor. Soc.*, **104**, 569–582.
- Kurihara, Y. and G. J. Tripoli, 1976: An iterative time integration scheme designed to preserve a low-frequency wave. *Mon. Wea. Rev.*, **104**, 761–764.
- Lin, S.-J., 1997: A finite-volume integration method for computing pressure gradient force in general vertical coordinates. *Quart. J. Roy. Meteor. Soc.*, **123**, 1749–1762.
- Lin, S.-J., W. C. Chao, Y. C. Sud, and G. K. Walker, 1994: A class of the van Leer-type transport schemes and its application to the moisture transport in a general circulation model. *Mon. Wea. Rev.*, **122**, 1575–1593.
- Matsuno, T., 1966: Numerical integrations of the primitive equations by a simulated backward difference method. *J. Meteor. Soc. Japan*, **44**, 76–84.
- Mesinger, F., 1977: Forward-backward scheme, and its use in a limited area model. *Contrib. Atmos. Phys.*, **50**, 186–199.
- Mesinger, F., Z. I. Janjić, S. Ničković, D. Gavrilov and D. G. Deaven, 1988: The step-mountain coordinate: Model description and performance for cases of Alpine lee cyclogenesis and for a case of an Appalachian redevelopment. *Mon. Wea. Rev.*, **116**, 1493–1518.
- Simmons, A. J. and D. M. Burridge, 1981: An energy and angular-momentum conserving vertical finite-difference scheme and hybrid vertical coordinates. *Mon. Wea. Rev.*, **109**, 758–766.
- Takacs, L. L. and R. C. Balgovind, 1983: High-latitude filtering in global grid-point models. *Mon. Wea. Rev.*, **111**, 2005–2015.

Wyman, B. L., 1996: A step-mountain coordinate general circulation model: Description and validation of medium-range forecasts. *Mon. Wea. Rev.*, **124**, 102–121.